Research Journal of Recent Sciences _____ ISSN 2277-2502
Vol. **4(1),** 55-61, January **(2015)** *Res.J.Recent Sci.*

Electrical and Structural Properties of WO_3-SnO_2 Thick-Film resistors Prepared by Screen Printing Technique

Garde A. S.
Material Research Laboratory, M.S.G. College Malegaon Camp and A.S.C. College Surgana, Nasik, 422211, University of Pune, MS, INDIA

Available online at: www.isca.in, www.isca.me
Received 28nd December 2013, revised 11th March 2014, accepted 4th May 2014

Abstract

WO_3-SnO_2 based thick films were prepared by using standard screen printing technique. The films were fired at optimized temperature of 600^0C for 30 minutes in air atmosphere. The material characterization was performed by XRD, SEM, and EDAX for elemental analysis. The UV-visible spectra show WO_3 -SnO_2 exhibits a shoulder at 232 nm along with an ill-defined band at 260 nm. The maximum optical band gap energy of 5.12 eV was obtained on a room temperature. The D.C. resistance of the films was measured by half bridge method in air atmosphere at different temperatures. The films were showing decrease in resistance with increase in temperature indicating semiconductor behaviour. The temperature coefficient of resistance (TCR), activation energy and sheet resistivity are evaluated at 600^0C.

Keywords: WO_3-SnO_2, Thick films, XRD, SEM, UV, activation energy, TCR.

Introduction

Microelectronics based on Thick and Thin film technologies, has shown rapid growth in the past few years and emerging as an important technique for miniaturization of electronic systems. The thin and thick film technologies have been going through several significant changes over the years.[1] The electrical properties of thick film resistors system are functions of several factors[2]. Such as ingredients, manufacturing technique and sintering history. The main ingredients of thick film include a conducting paste, such as an oxide powder; dielectric phase, such as glass frit; and an insulating substrate, such as alumina. The oxides used in thick films can be broadly classified into two groups: metallic where the resistivity usually obeys a power law dependence on temperature, $\rho \alpha T^n$, where $n \geq 0$ and semiconducting, where the resistivity usually follows an exponential law, $\rho \alpha e^{(E/KT)}$. Hybrid Several deposition methods have been used to grow undoped and doped WO_3 films such as Spray Pyrolysis, Evaporation, Chemical vapour deposition, electrochemical deposition, Magnetron Sputtering, Pulsed Laser deposition, a Sol Gel technique and a screen printing technique[3]. The screen printing technique was introduced in the later part of the 1950's to produce compact, robust and relatively inexpensive hybrid circuits for many purposes and it is a viable and economical method to produce thick films of various materials[4,5]. Today our environment is polluted by number of gases exhausts from auto and chemical industry. In order to detect measure and control the gases one should know the amount and type of gases present in the ambient. Therefore the need to monitor and control these gases has led to the research and development of very large variety of sensors using different materials and technologies. Sensors play an important role in the areas of emissions control, environment protection, public safety, and human health[6,7]. Much more public concern today than ever before over serious environmental issues is further promoting the development of sensors with both high sensitivity and rapid response. Metal oxide semiconductor materials such as SnO_2, ZnO, TiO_2, WO_3, V_2O_5, Fe_2O_3, ZrO_2, CeO_2, In_2O_3, Cr_2O_3, $BaTiO_3$, Ga_2O_3 etc. have been well reported as gas sensors in the form of thick film[8]. The use of sensors or resistors is basically for industrial process controls, in human health and for the prevention of hazardous gas leaks, measurements of physical quantities and for controlling some systems, which comes from the manufacturing processes[9]. There are many types of gas sensors that have been used to detect various gases: catalytic gas sensors, infrared gas sensors, semiconductor gas sensors etc.

Tungsten is the third element in group VI B of the Periodic Table. It Possesses different oxidation states ranging from (0) to (+VI) in various inorganic compounds. WO_3 has the oxidation state (+VI), its density is higher than Cr and Mo which is found in its group[10]. Tungsten oxide possesses a polycrystalline structure with a wide band gap semiconductor. Its band gap energy has been mainly by optical absorption varying from about 2.6-3.0 eV. The most common structure of WO_3 is monoclinic with space group $P2_1/n$. WO_3 films are reported to have promising electrical and optical properties for various applications like efficient photolysis, electrochromic devices, selective catalysts and gas sensors[11,12]. Amorphous and polycrystalline WO_3 films are particularly attractive as gas sensors because they show a catalytic behavior both in oxidation and reduction reaction[13]. Electro chromic devices which exploit WO_3 are typically in an amorphous form, whereas electrical devices such as gas sensors are in a crystalline form[14]. Tungsten also forms other oxides such as WO, W_2O_3 and W_4O_3, however in gas sensing the stable WO_3 form is used. Tungsten Oxide is known to be a very promising

candidate good selectivity for sensing of the air pollutants NO/NO_2, CO/CO_2 and ethanol[15,16]. The sensing behaviour of bulk WO_3 is known to be a function of its chemical and physical properties such as Surface area, phase composition, crystallinity, and stoichiometry. Generally, the majority of the WO_3 sensing properties are connected with:(1) the WO_3 structural model is perovskite-type ABO_3 lattice with A site, which remains unoccupied site: (2) The WO_3 is considered as oxygen-deficient or non-stoichiometrical oxides. Additionally, it is accepted that the sensitivity is mainly influenced by the sensing material. The advantages of the resistors fabricated by WO_3 are simple design, long term stability, small size, light weight, low cost, good mechanical strength, high reliability, fast response. However, WO_3 gas sensors have good sensitivity at high temperature between 200 and 500^0C[17,18]. Tin oxide possesses a rutile structure (six atoms per tetragonal unit cell) with a wide band gap of semiconductor (Eg = 3.6 eV). The band structure of the n-type tin oxide has been calculated several times using tight binding method based on oxygen 2s and 2p orbital and tin 5s and 5p orbital[19,20,21]. The SnO_2 based gas sensors are used because of their long term stability, small size, light weight, low cost, good mechanical strength, high reliability, fast response to the gas. The aim of present work is to prepare WO_3-SnO_2 thick films by standard screen printing technique on alumina substrate and to investigate their electrical and structural properties fired at 600^0C.

Material and Methods

Powder, Paste and Thick Film Preparation: Commercially available white color WO_3 (Loba Chem.) and SnO_2 powder (Loba Chem.) is mixed thoroughly in an acetone medium by using a mortar and pestle with a permanent binder (lead borosilicate glass frit with a composition of 70 wt.% PbO, 18 wt.% SiO_2, 3 wt.% Al_2O_3, 3 wt.% B_2O_3 and 6% TiO_2)[22]. Initially the fine powder calcinied at 450^oC for 2 hour in muffle furnace. The pastes used in screen- printing were prepared by maintaining inorganic to organic materials ratio at 70:30. The inorganic part consisted to a functional material WO_3, additive SnO_2 and glass frit (in ratio of 85:10:5). The organic part consisted of 8% ethyl cellulose (EC) and 92% butyl carbitol acetate (BCA). A solution of EC +BCA (in ratio of 8:92) was made and added dropwise to the WO_3-SnO_2 mixture until proper thixotropic properties of paste were achieved. The paste was screen printed onto an alumina substrate (96% pure Kyocera). The details of the technique are described elsewhere[23]. The films were dried under IR lamp for 1 hour in an air to remove the organic binder and fired at 600^0C for 30 minutes in the muffle furnace for better adhesion. During the firing process glass frit melts and the functional materials are sintered. The function of glass frit is to bind grains together.

Thickness Measurements: The thickness of the WO_3-SnO_2 thick films were measured by using Taylor-Hobson (Taly-step UK) system. The thickness of the films was observed in the range of 15-18 μm.

Material Characterizations: The WO_3-SnO_2 thick film material is characterized by X-ray diffraction technique [Miniflex Model, Rigaku-Japan, DMAX-2500, CuKα (λ=1.542AU) radiation] for structural analysis, degree of crystallinity and grain size determination for Braggs angle (2θ) from 20 to 80 degree. The average grain size was determined by using Debye Scherer formula. [24]

$$D = \frac{0.9\lambda}{\beta \cos\theta} \quad (1)$$

Where D is the grain size, λ is the wavelength of the X-ray radiation (1.542 AU), θ is the angle of diffraction and β is the full angular width of diffraction peak at the half maximum peak intensity.

Surface Morphology of the WO_3-SnO_2 thick films were studied by using scanning electron microscopy, SEM, (JOEL JED-2300, Japan) with Energy Dispersive Analysis of X-rays, EDAX for chemical composition. The Ultraviolet and visible optical absorption spectra were measured in the range 200–800 nm. A recording spectrophotometer (JASCO UV-VIS-NIR Model No.V-670) was used for these optical measurements.

Electrical Characterization: The DC resistance of the film samples was measured by half bridge method with a function of temperature in atmosphere[25]. Sheet resistivity (ρ_s) was determined for each of the samples. Sheet resistivity (ρ_s) = ρ/t, where ρ = resistivity of thick film resistor, t = thickness of the film resistor in micrometers. The effect of temperature on the resistance was studied to determine the temperature coefficient resistance (TCR) and calculated as

$$TCR = \frac{1}{R_o}\left(\frac{\Delta R}{\Delta T}\right) / ^o C \quad (2)$$

Where ΔR = change in resistance between temperature T_1 and T_2 , ΔT = temperature difference between T_1 and T_2, R_o = Initial resistance of the film sample.

The activation energy of thick film resistors was calculated by the Arrhenius plot using the relation

$$R=R_o e^{-\Delta E/KT} \quad (3)$$

Where R_o= the constant, ΔE=the activation energy of the electron transport in the conduction band, K=Boltzman constant and T=Absolute temperature.

Result and Discussion

X-ray diffraction analysis of WO_3-SnO_2 thick film: Figure-1 Shows an XRD patterns pure WO_3 and WO_3-SnO_2 thick film samples fired at 600^0C plotted in the range 20-80^0 (2θ). The XRD pattern shows several peaks of tungsten oxide and tin oxide phases indicating polycrystalline nature. The observed

peaks of WO_3 and SnO_2 match well with reported ASTM data confirming polycrystalline structure. The sharp peaks reflexes seen on the pattern indicate that a transformation to a highly ordered crystallite has occurred in the material. The higher peak intensities of an XRD pattern is due to the better crystallinity and bigger grain size can be attributed to the agglomeration of particles. It is observed that as the firing temperature, the major contribution towards monoclinic phase also present as shown in table 1.

Figure-1 shows that the diffraction peaks of WO_3 at 2θ values of 23.7^0, 24.2^0,25^0,34.7^0 and 56.4^0 which reveals the formation of the Monoclinic phase [ASTM Card No.43-1035], peaks at 34.5^0 reveals the formation of Triclinic phase[ASTM Card No.32-1395], peaks 28.0^0, 50.5^0,62.8^0, and 77.7^0 reveals the formation of Hexagonal phase [ASTM Card No.33-1387]. Peak 33.9^0 reveal the formation of Cubic phase [ASTM Card No.46-1096]. Peaks of SnO_2 at 51.2^0, 58.2^0 and 62.4^0 reveal the formation of Tetragonal phase [ASTM Card No.21-1250] and 42.4^0 reveal the formation of Orthorhombic phase [ASTM Card No.24-1342]. Some peaks of Al_2O_3 are due to the alumina substrate. The average grain size for the film sample is calculated by Scherer formula [24] were found to be 56.72 nm (± 2nm) at 600^OC (±2 ^OC) respectively.

Table-1
Illustrates the Presence of % Relative Phases of WO_3-SnO_2Thick Film Resistor Fired at 600^0C

% of relative presence of phases						
M-WO_3	Tr-WO_3	C-WO_3	H-WO_3	T-SnO_2	O-SnO_2	Al_2O_3
37.23	10.80	5.40	16.85	9.96	7.65	12.11

Micro Structural Analysis by SEM: Figure-2 Shows the SEM micrographs of WO_3-SnO_2 thick films for studying the surface morphology. The SEM micrographs of WO_3 thick films fired at 600^0C shows polycrystalline structure with number of pores (voids) distributed on the surface of the film, basically due to evaporation of organic binder during the firing of the films. The particle size of WO_3-SnO_2 thick film is 320 nm (±2nm) at 600^0C (±2^0C).The average particle size observed in SEM is much higher than estimated from bulk XRD data, indicating agglomeration of the particles.

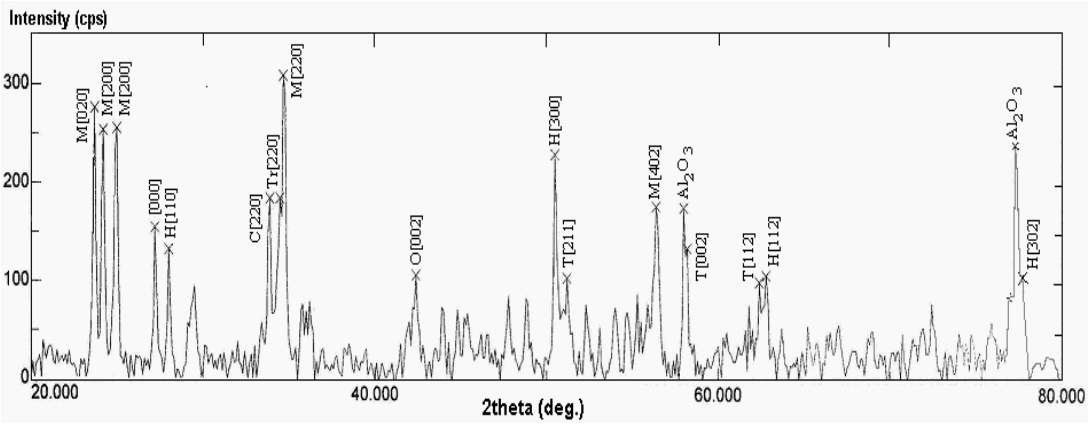

Figure-1
XRD pattern of WO_3-SnO_2 thick films fired at 600^0C

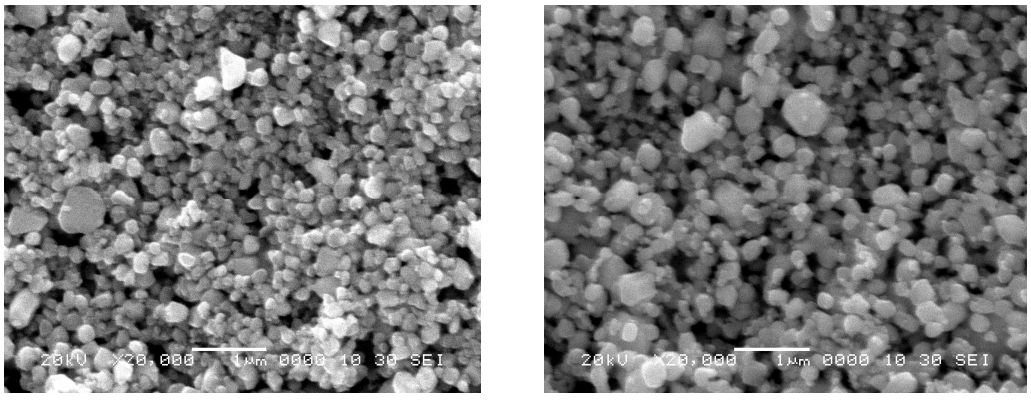

(a) (b)

Figure-2
Scanning Electron Micrograph of WO_3-SnO_2 Thick films (a) unfired and (b) fired at 600^0C Elemental analysis

The EDAX analysis of WO_3-SnO_2 thick films showed presence of only W, Sn and O as expected, no other impurity elements were present in the WO_3-SnO_2 film samples. Also from the EDAX spectra, it is found that wt% and at% of W, Sn and O are nearly matched illustrate in table- 2.

Table-2
Composition of the WO_3-SnO_2 thick films fired at 600^0C

Wt %	Mass %	At %	Error %
W	68.82	33.82	0.54
Sn	22.50	17.12	0.62
O	8.69	49.06	0.57

Optical studies: Figure-3 shows the optical absorbance spectra of pure WO_3 and WO_3-SnO_2 powder sintered at 450^0C in the wavelength range 200–800 nm. From figure it is seen that the UV spectrum of pure WO_3 and WO_3-SnO_2 exhibits a shoulder at 230 and 232 nm along with an ill-defined band at 260 nm. The variation of optical density with wavelength was analyzed to find out the nature of transition involved and the optical band gap. The wavelength at which 'α' rises suddenly corresponds to the band gap energy that was estimated. The absorption coefficient is found to be 4.0 supporting the presence of direct band gap.[26]

The nature of the transition is determined by using the Tauc relation-4 [27]

$$\alpha = A\,(h\nu - E_g)^{1/2}/h\nu \qquad (4)$$

Where *Eg* is the optical band gap energy, *A* is a constant. The plot of $(\alpha E)^2$ as a function of the Photon energy ($h\nu$) of the incident radiation has been shown in Figure-4 a and Figure-4 b.

It is found that the plot is nonlinear indicating absence of indirect transition. The band edge can be evaluated from the intercept of the extrapolated linear part of the curve with the energy axis. The optical band gap of WO_3-SnO_2 is estimated to be 5.12 eV and pure WO_3 is estimated to be 4.85 eV which is larger than the reported value[28]. The difference in present case may be attributed to the different mechanism and technique.

The DC resistance of the WO_3-SnO_2 thick films fired at 600^0C ($\pm 2^0$C), were measured by using half bridge method as a function temperature. The resistance of thick films decreases with increase in temperature showing semi conducting behavior.

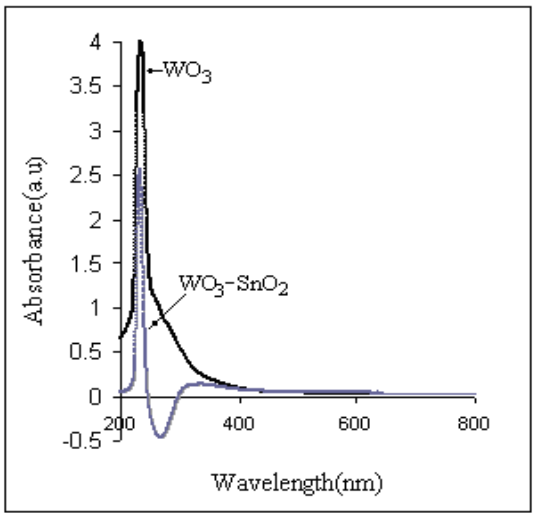

Figure-3
Absorption spectra of pure WO_3 and WO_3-SnO_2 powder sintered at 450^0C

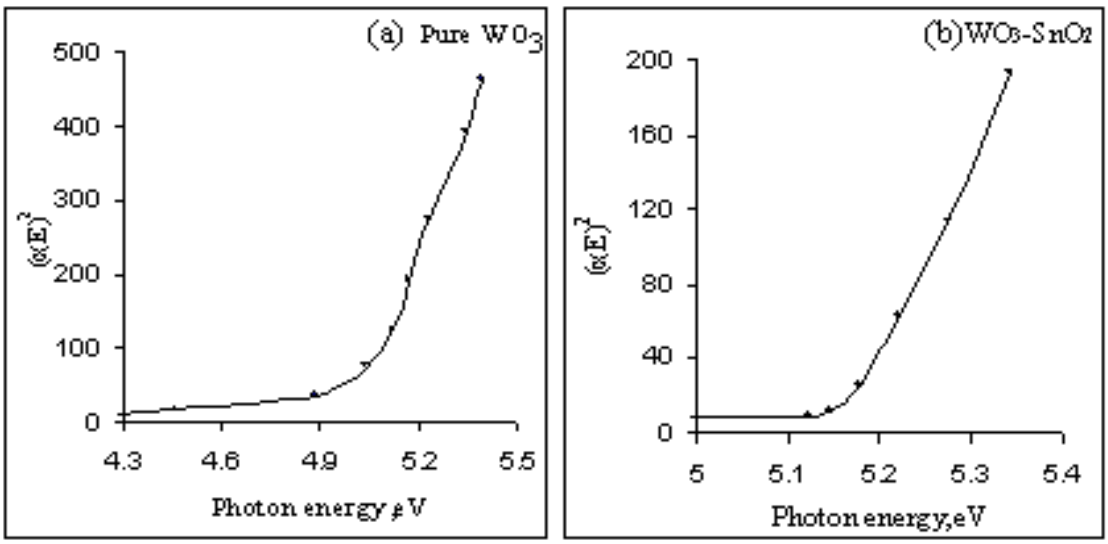

Figure- 4
Plots of $(\alpha E)^2$ against Photon energy for (a) pure WO_3 and (b) WO_3-SnO_2 powder sintered at 450^0C

Electrical characterization

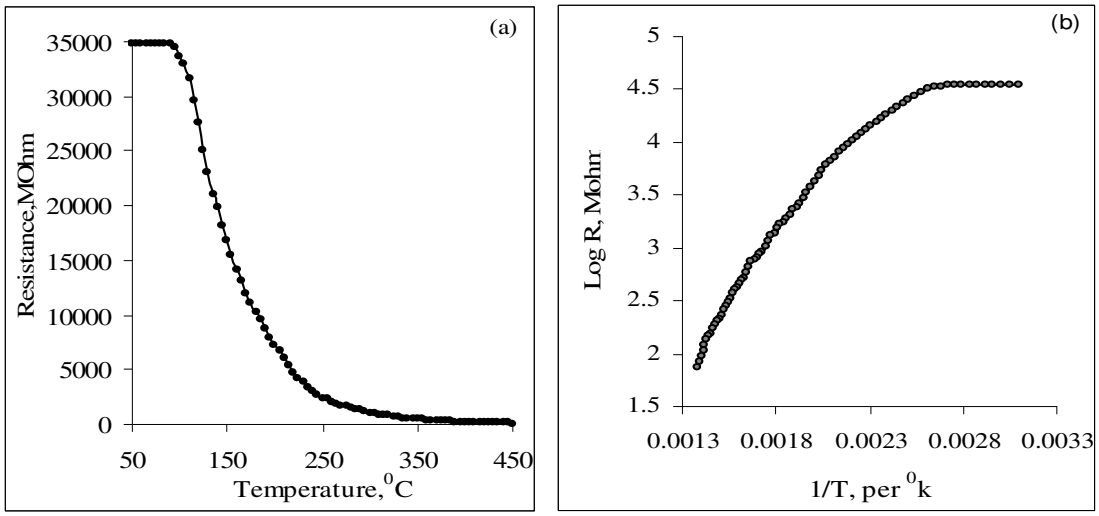

Figure-5
Variation of (a) Resistance with temperature and (b) Log R with reciprocal of temperature of WO_3-SnO_2 thick films fired at 600^0C

Figure-5 a shows the resistance variation of WO_3-SnO_2 thick films fired at 600^0C (± 2 ^{0}C) temperatures in air. SnO_2 doped Tungsten oxide thick film samples exhibited three regions of resistance similarly to pure SnO_2 thick film Sensors[29]. The plot shows different conduction region: (i) continuous fall of resistance, (ii) an exponential fall region and (iii) finally saturation region. Any increase in temperature of thick film causes the electrons to acquire enough energy and cross the barrier at grain boundries[30,31]. There can be decrease in potential barrier at grain boundries, since at higher temperature the oxygen adsorbates are desorbed from the surface of the films. There is a decrease in resistance with increase in temperature indicating semiconducting behavior, obeying $R=R_O e^{-\Delta E/KT}$ in the temperature range of 50 to 450^0C. For WO_3 –SnO_2 film samples fired at 600^0C, initially resistance is constant up to 90^0C temperature, and then falls linearly up to a certain transition temperature. After the transition temperature the resistance decreases with exponential fashion and finally saturate to steady level. The transition temperature depends on firing temperature of the film. The initially value of WO_3-SnO_2 thick film resistance in air atmosphere (at 50^0c) was 34873, Mohm fired at 600^0C respectively.

Figure-5b shows log R versus reciprocal of temperature (1/T) variation of WO_3-SnO_2 thick films fired at 600^0C. This variation is reversible in both heating and cooling cycles obeying the Arrhenius equation $R=R_o e^{-\Delta E/KT}$ where, Ro= the constant, ΔE = the activation energy of the electron transport in the conduction band, K =Boltzman constant and T =Absolute temperature. It is seen that the curve has two distinct regions of temperature namely low temperature region (323 to 458 ^{0}K) and high temperature region (638 to 723 ^{0}K). The activation energy in the lower temperature region is always less than the energy in the higher temperature region because material passes from one conduction mechanism to another. The earlier reported activation energy value of pure WO_3 is 0.82 eV[32]. In low temperature region, the increase in conductivity is due to the mobility of charge carriers which is dependent on the defect/dislocation concentration. So, the conduction mechanism is usually called the region of low temperature conduction. In this region activation energy decreases, because a small thermal energy is quite sufficient for the activation of the charge carriers to take part in conduction process. In other words the vacancies/ defects weakly attached in lattice can easily migrate (extrinsic migration). Hence increase in the conductivity in the lower temperature region can be attributed to the increase in charge mobility. In high temperature region, the activation energy is higher than that of low temperature region. In this region the electrical conductivity is mainly determined by the intrinsic defects and hence is called high temperature or intrinsic conduction. The high values of activation energy obtained for this region may be attributed to the fact that the energy needed to form defects much larger than the energy required for its drift. For this reason the intrinsic defects caused by the thermal fluctuations determine the electrical conductance of the film samples only at elevated temperature. The value of grain size, sheet resistivity, temperature coefficient resistance and activation energy of the WO_3-SnO_2 thick films fired at temperatures of 600^0C is summarized in table-3.

Table-3
Grain size, TCR, Sheet resistivity and Activation energy of WO_3-SnO_2 thick films fired at 600^0C [Thickness:-16µm]

Grain Size (nm)	TCR, x 10^{-3} ($/^0$C)	$\rho_s x10^{12}\Omega/\square$	Activation energy, eV	
			Low T.R	High T.R
56.72	4.458	0.02179	0.12206	0.74758

Conclusion

WO_3-SnO_2 thick films deposited on alumina substrate using screen printing technique were showing semiconductor behaviour. XRD analysis shows the structure of WO_3-SnO_2 films is polycrystalline in nature. The higher peak intensities of an XRD pattern is due to the better crystallinity and bigger grain size can be attributed to the agglomeration of particles. The activation energy in the lower temperature region is always less than the energy in the higher temperature region. It also shows voids between the particles basically due to evaporation of the organic solvent during the firing of the films. From optical studies, the direct band gap value of pure WO_3 and WO_3-SnO_2 was found to 4.85 and 5.12 eV respectively. The UV-visible spectrum of pure WO_3 and WO_3-SnO_2 exhibits a shoulder at 230 and 232 nm along with an ill-defined band at 260 nm respectively.

Acknowledgement

The authors are grateful to Management authorities of M.G. Vidyamandir's, Malegaon (Nasik) for providing laboratory facilities for doing the work and also thankful to Dr. R Y Borse for their fruitful suggestions on the subject of paper. Authors sincerely thank U.G.C. for financial assistance for this research project.

References

1. Short term course on Thick and Thin film hybrid Microelectronics, Indian institute of science, Bangalore, September, **(1986)**

2. Anisur Raheman K.M., Susan Schneider and Seitz Martin, Hopping and Ionic conduction in Tin Oxide Based Thick-Film Resistor Compositions, *J.Am.Ceram. Soc*., **80,** 1198-1202 **(1997)**

3. Joseph Benny, Gopchandran K.G, Manoj P.K., Peter koshy Manoj, and Vaidyan V.K., *Bull. Mater. Sci.,* **22,** 921-926 **(1999)**

4. Ansari S.G, Boroojerdian P., Sainkar S.R, Karekar R.N, Aiyer R.C and Kulkarni S.K, Effect of Thickness on H_2 Gas Sensitivity of SnO_2 Nanoparticles Based Thick Film resistors, *J. of Materials Science: Materials in Electronics*, **7,** 267-270 **(1996)**

5. Patil L.A, Wani P.A, Sainkar S.R, Mitra A., Pathak G.J and Amalnerkar D.P, Studies on fritted thick films of photo conducting Cds, *Materials Chemistry and Physics*, **55,** 79-84 **(1998)**

6. Kolmakov A. and Moskovits M., Chemical Sensing and Catalysis by one Dimensional Metal Oxide Nanostructures, *Ann Rev. Mater. Res*., **34,** 151-180 **(2004)**

7. Park Jinsoo, Shen Xiaoping and Wang Guoxiu, Solvothermal synthesis and gas sensing performance of CO_3O_4 hollow nanospheres, *Sensors and Actuators,* **B 136,** 494-498 **(2009)**

8. Guidi V., Butt Uri M.A, Carrotta M.C and Cavicchi B., Gas sensing Through Thick Film Technology, *Sensors and Actuators, **B*** **84,** 72-77 **(2002)**

9. More P.S, Karekar R.N, Deshpande S., Sali N.D, Bhoraskar S.V, Sainkar S. and Aiyer R.C, Introduction of ∂-Al_2O_3/Cu_2O Material for H_2 gas Sensing Applications, *Material Letters*, **58,** 1020-1025 **(2004)**

10. Ouis M.A, El-Batal H.A, Azooz M.A and Abdelghany M.A, Characterization of WO_3- doped borophosphate glasses by optical, IR and ESR Spectroscopic Techniques before and after subjecting to gamma irradiation, *Indian Journal of Pure & Applied Physics*, **51-1,** 11-17 **(2013)**

11. Granqvist C.G in Handbook of Inorganic Electrochromic Materials, Elsevier Amsterdam, **(1995)**

12. Sun H.T, Cantalini C., Lozzi L, Passacantando M. & Santucci S, Microstructural effect on NO_2 sensitivity of WO_3 thin film gas sensors.Part I. *Sensors and Actuators*, **287,** 258-265 **(1996)**

13. Kung H.H, Transition Metal Oxides: Surface Chemistry and catalysis, Elsevier, NY, **(1989)**

14. Takase A. and Miyakawa K., Raman study on sol-gel derived tungsten oxides form tungsten ethoxide, *Jpn. J. Appl. Phys*., **30 (8),** 1508-1511 **(1991)**

15. Ahmed F, Nicoletti S, Zampolli S and Elmi, *Sensors and Microsystems in Proceedings of the 7th Italian Conference, Bologna, Italy* **4-6 (2),** 197-203 **(2002)**

16. Sberveglieri G. Depero L., Groppelli S, and Nelli P, WO_3 sputtered thin films for NOx monitoring, *Sensors and Actators,* **B 26-27,** 89-92 **(1995)**

17. Sun H.T, Cantalini C., Lozzi L, Passacantando M. & Santucci S, Microstructural effect on NO_2 Sensitivity of WO_3 thin film gas sensors.Part I. *Sensors and Actuators*, **287,** 258-265 **(1996)**

18. Solis J.L, Sukko S, Kish L.B, Granqvist C.G and Lantto V, Nano-crystalline Tungsten Oxide Thick Films with High sensitivity to H_2S at Room Temperature, *Sensors and Actuators,* **B77,** 316-321 **(2001)**

19. Robertson J., Electronic structure of SnO_2, GeO_2, PbO_2, TeO_2 and MgF_2, J. *Phys., **C*** **12**, 4767-4776 **(1979)**

20. Munnix S and Schmeits M., Electronic structure of Tin Oxide Surfaces, *Physics Review* **B 27**, 7624-7635 **(1983)**

21. Munnix S. and Schmeits M., Electronic structure of point defects on oxide surfaces, *Physics Review, **B*** **33**, 4136-4144 **(1986)**

22. Maissel L.I and Glang R. (Eds.), Hand book of thin film technology, McGraw-Hill, New York, (**1974**)

23. Garje A.D and Aiyer R.C, Electrical and Gas-sensing

Properties of a thick film Resistor of Nanosized SnO_2 with variable Percentage of permanent binder, *Int. J. Appl. Ceram. Technol.*, **3(6)** 477-484 **(2006)**

24. Cullity B.D, *Elements of X-ray diffraction*, *Addison-Wesley Publishing Co*. **(1956)**

25. Sarladevi G,.Manoramma S. and Rao V.J., Gas sensitivity of SnO_2/CuO heterocontact, J. *Electrochem.soc.*, **142(8),** 2574-2577 **(1995)**

26. Desai J.D and Lokhande C.D, *Mate. chem. Phys.,* **34,** 313-316 **(1993)**

27. Okoil L.U, Ozuomba J.O and Ekpunobi A.J., Influence of Local Dye on the Optical band-gap of Titanium Dioxide and its performance as a DSSC Material, *Res. J. of Phy. Sci.,* Vol. **1(10),** 6-10, **(2013)**

28. Washizu E., Yamamoto A, Optical and Electrochromic Properties of RF reactively sputtered WO_3 Films *Solid State Ionics*, **165(1-4),** 175-180 **(2003)**

29. Chiorino A., Ghiotti G, Prinetto F., Carotta M.C, Malagu C., Martinelli G, Electrical and Spectroscopic Characterization of SnO_2 and Pd-SnO_2 Thick Films studied as CO Gas Sensors, *Sensors and Actuators*, **B 47,** 205-212 **(1998)**

30. Borse R.Y and Garde A.S, Effect of Firing temperature on electrical and structural characteristics of SnO_2 thick films. *Indian J Phys.,* **82 (10),** 1319-1328 **(2008)**

31. Windichmann H. and Mark P.A, Model for the Operation of a Thin-Film SnO_x conductance- Modulation Carbon Monoxide Sensor, *J. Electrochem. Soc*., **126,** 627-633 **(1979)**

32. Mohammad A. Al., Synthesis separation and electrical properties of WO_3-x Nan powders via partial pressure High Energy Ball-Milling, *Acta Physica Poloncia,* Vol. **116,** 240-244 **(2009)**